J Mater Sci: Mater Med (2010) 21:2079–2085
DOI 10.1007/s10856-010-4084-7

Evaluation of the stress distribution in CFR-PEEK dental implants by the three-dimensional finite element method

João Rodrigo Sarot · Cintia Mussi Milani Contar · Ariadne Cristiane Cabral da Cruz · Ricardo de Souza Magini

Received: 12 August 2009 / Accepted: 15 April 2010 / Published online: 13 May 2010

Abstract CFR-PEEK (carbon fiber reforced—poly ether ether ketone) has been demonstrated to be excellent substitute titanium in orthopedic applications and can be manufactured with many physical, mechanical, and surface properties, in several shapes. The aim of this study was to compare, using the three-dimensional finite element method, the stress distribution in the peri-implant support bone of distinct models composed of PEEK components and implants reinforced with 30% carbon fiber (30% CFR-PEEK) or titanium. In simulations with a perfect bonding between the bone and the implant, the 30% CFR-PEEK presented higher stress concentration in the implant neck and the adjacent bone, due to the decreased stiffness and higher deformation in relation to the titanium. However, 30% CFR-PEEK implants and components did not exhibit any advantages in relation to the stress distribution compared to the titanium implants and components.

J. R. Sarot (✉)
Department of Pos-Graduation Course of Implantology, Universidade Federal do Paraná, Curitiba, Brazil
e-mail: sarotimplantes@terra.com.br

C. M. M. Contar
Department of Oral Radiology, Universidade Tuiuti do Paraná, Curitiba, Brazil

A. C. C. d. Cruz
Biotecnology Post-Graduation Program, Universidade Federal de Santa Catarina, Florianópolis, Brazil

R. de Souza Magini
Department of Denstistry, Universidade Federal de Santa Catarina, Florianópolis, Brazil

1 Introduction

The field of implantodontics has experienced significant advancements over the past 40 years, which have revolutionized the field and resulted in paradigm shifts in the search for solutions and improvement in the buccal whitewashing technology. Certain topics in implantodontics are of prime concern, such as implant amount, shape, surface treatment, and the esthetics of prosthetic components, and have been widely discussed. The use of polymers to manufacture bone-integrated implants as a substitute for conventional titanium components has also been developed [1].

PEEK (poly-ether-ether-ketone), which is a dominant member of the PAEK (poly-aryl-ether-ketone) polymer family, appeared during the 1990s as a main substitute for the metallic components and implants of high-performance thermoplastic polymers, especially in cases of orthopedics and trauma. The growing interest in poly-aromatic polymers is evident in the development of hip prostheses and plates for fracture fixation that are of similar stiffness to bone [2, 3]. Although pure poly-aromatic polymers exhibit an elastic modulus that varies from 3 to 4 GPa, this value can be modified to achieve a close module to cortical bone (18 GPa) with the addition of composites, such as carbon fiber (CFR-PEEK) [4]. This biocompatible material [5–10] can be performed with a wide range of physical, mechanical, and surface properties and in several shapes and it provides many possibilities in the development of new implants and components for buccal whitewashing, particularly due to the biomechanical behavior of this material. Based on the energy dissipation theory [11], a force applied to the implant-supported crown is known to be transferred through the implant, with small alterations due to the energy conservation feature of the rigid implants, which results in an elastic deformation and minimal mechanical energy storage by the

implant. Metallic implants are at least eight times harder than the neighboring bone. This gradient difference generates stress in the bone-implant interface during load transfer. An implant with an elastic modulus similar to bone suggests the potential for a more homogenous stress distribution to the support tissues with a stress decrease in this interface.

The aim of this study was to compare, using the Finite Elements Method (FEM), the stress distribution near the peri-implant bone in four distinct models composed of titanium abutment with implant, CFR-PEEK abutment with titanium implant, titanium abutment with CFR-PEEK implant, and CFR-PEEK abutment with implant.

2 Material and method

A randomly chosen computerized tomography exam (i-CAT, Xoran Technologies, Ann Arbor, USA) was used to obtain the digital model in the initial phase of the work. The tomography exam was performed on the third front bottom part of the face to analyze the jaw region in transversal slices of 0.25 mm in length, a total of 212 slices. These slices were recorded in Dicom format (Digital Imaging and Communications in Medicine Standard) and imported to an image processing and digital reconstruction program (software developed by the post graduation course in Numeric Methods and Engineering of Universidade Federal do Paraná, Brazil). This program was utilized to digitally reconstruct the jaw and the result was a 3D model. Only the part portion corresponding to tooth number 35 was extracted from this model.

After the virtual reconstruction, the 3D model was exported to the Ansys DesignModeler v11 software (Ansys Inc., Canonsburg, PA, USA) in the virtual models edition. An unitary implant, prosthetic components (abutment and bolt), as well as cortical and medullar bone around the implant were modeled. The previously scanned tooth was cut in the cervical portion and bonded to the model in order to represent a prosthetic crown bonded to the implant according to the specifications described below (Fig. 1).

Implant, *abutment* and screw:

- Screwed cylindrical implant with a hexagon connection, 10 mm in height and platform diameter of 4.1 mm.
- Universal abutment with an outer hexagon type connection, 4.1 mm bottom platform and upper conic portion.
- Titanium bolt with screws only in the lower third.

Prosthesis:

- Chrome-cobalt structure that was at least 0.3 mm thick on the implant *abutment* and with a similar shape to the ceramic crown.

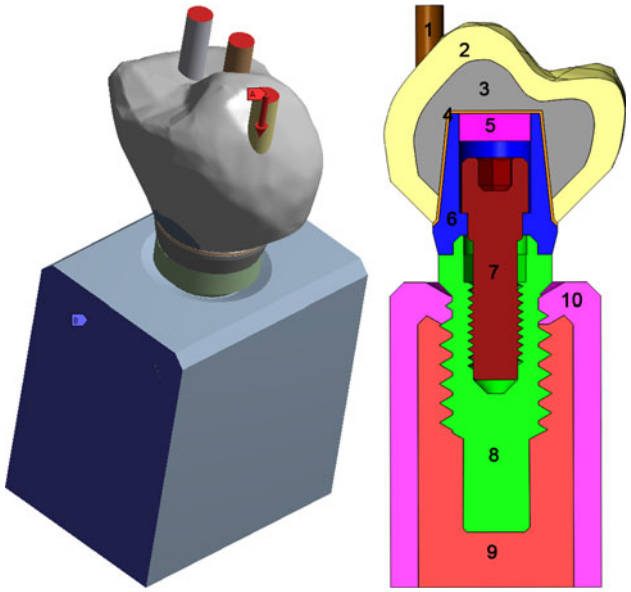

Fig. 1 Figure of the final model with cylinders enamel in order to simulate dental contacts. Explicative cut on the right: 1—enamel cylinder; 2—feldspatic porcelain; 3—chrome-cobalt structure; 4—zinc phosphate cement; 5—guta percha; 6—universal abutment with an outer hexagon type connection; 7—titanium bolt with screws in the lower third; 8—screwed cylindrical implant with a hexagon connection; 9—medullar bone; 10—cortical bone

- Feldspatic porcelain covering the structure and modeling the coronary shape of the prosthesis.

Other structures:

- A zinc phosphate line that was approximately 0.1 mm thick and located between the connector and prosthesis.
- Guta-percha for bolt protection.
- Cortical bone of 1.0 mm thick covering the bone crest.
- Medullar bone covering the inner portion of the cortical bone.

The different models of this work, described in Table 1, aimed to evaluate the impact of stresses on the CFR-PEEK components and implants reinforced with 30% carbon fiber on a unitary implant treatment.

All models were identical, except for the properties of the used materials, and all were exported from the DesignModeler software (Ansys Inc., Canonsburg, PA, USA) to the Ansys Workbench V11 finite elements simulation software (Ansys Inc., Canonsburg, PA, USA). Each

Table 1 Characteristics of the different tested models

Model	Implant	Abutment
A	Titanium	Titanium
B	Titanium	CFR-PEEK
C	CFR-PEEK	Titanium
D	CFR-PEEK	CFR-PEEK

Table 2 Mechanical properties of the materials

Material	Young modulus (MPa)	Poisson ratio
Guta percha [26]	0.69	0.45
Enamel cylinder [27]	84100	0.20
Cortical bone [28]	17400	0.30
Medullar bone [28]	1740	0.30
Zinc phosphate cement [26]	22400	0.25
Feldspatic porcelain [29]	69000	0.30
Titanium (implant, bolt, abutment) [30]	110000	0.35
30% CFR-PEEK [6, 31]	18000	0.39
Crome-cobalt structure [32]	218000	0.33

element from the models was configured with an elastic modulus and the Poisson ratio was determined from the literature according, to the simulated model (Table 2). All contacts among the structures were considered perfect bonded, except for the bonding between the zinc phosphate cement and the abutments. The contacts between titanium and CFR-PEEK universals abutments and zinc phosphate cement were considered frictional, which allow for slides and space formation in order to approach a real situation. Zinc phosphate cement doesn't have real bonding effect, only mechanical retention [12]. Although friction coefficients vary according to several factors, a 0.2 coefficient was used based on other similar materials [13] for the bonding between zinc phosphate cement and titanium abutment as well as between zinc phosphate cement and CFR-PEEK. The simulations were non-linear in relation to the contact.

Rigid supports were added in the lower and lateral regions of bone to simulate the bonding of the model to the rest of a jaw. Vertical and oblique (30°) loads in relation to the long axis of the tooth with 100 N in magnitude were applied. The meshes were validated through a refinement process of the mesh, checking and the convergence of results was verified. When the difference between the stress peaks of the results reached a predetermined error of 5% or less, the mesh was considered valid. The mesh was created with tetrahedral elements (Fig. 2), resulting in meshes with 1,402,615 nodes and 894,630 elements. All models were then solved (Windows XP X64, Intel Core 2 quad Q6600 processor, 8 Gb of RAM memory), and the graphic and numeric plotting of the data was registered, evaluated, and compared. Stress analysis was performed by comparing the compression stress and Von Mises stress components. The Von Mises stress [14] is a criterion that includes all stress components on the implants, including shearing. An analysis of the models' deformation degree was also performed in the same simulation using the same software.

3 Results

The results are presented in stress/strain diagrams, with the stress distribution for qualitative evaluation and in numeric values of the stress peaks for quantitative evaluation. The compression load had a similar behavior for the four models, indicating the predominance of the implant shape in the load distribution pattern. The CFR-PEEK implants (models C and D) presented a higher load concentration in the cervical portion and on the cortical bone than the titanium implants (models A and B). The abutment materials did not result in any interference with this result (Fig. 3). The tensile loads exhibited lower intensity than the compression loads, and there was no significant difference in the distribution pattern among the different models (Table 3).

For the Von Mises stress, the titanium implants (models A and B), presented equivalent stress peaks in the cervical portion and a more homogeneous load distribution throughout the implant body. However, the CFR-PEEK implants (models C and D) presented more concentrated stress in a smaller portion of the cervical area, which did not take full advantage of the implant length. Similarly to the implants, the titanium abutments (models A and C) had a more homogeneous stress distribution with equivalent stress peaks. In models C and D, the CFR-PEEK abutments resulted in similar behaviors as the CFR-PEEK implants, concentrating the loads in a smaller area (Fig. 4). The total deformation analysis demonstrated a lower deformation peak of model A (titanium implant and abutment) and a higher deformation in the model D (CFR-PEEK implant and abutment), (Fig. 5). Table 3 presents the stress peaks in the different structures of the models relative to the simulations presented in Figs. 3 and 4 for quantitative analysis. Table 4 shows the stress peaks in a simulation with the load applied in the oblique direction on the crown.

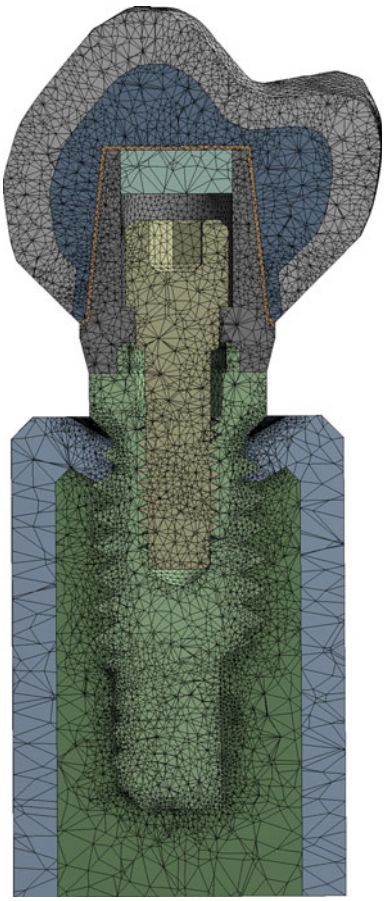

Fig. 2 Mesh of the complete model. The mesh was refined in order to present higher density in the important regions for this study

4 Discussion

The promising mechanical properties of the PEEK polymer family coupled to the enormous versatility in shapes and applications of such implants has resulted in great interest in these biomaterials, since the 1990s. Until these developments, the best-achieved results in medicine were reported in orthopedics, particularly in the spine field with the use of cages for intervertebral stabilization [15]. Other studies [16–18] have also demonstrated favorable clinical performance of this polymer in orthopedic patients. These results are attributed to similarity of the elastic modulus to the bone, which is a feature of the PEEK reinforced with 30% carbon fiber. Therefore CFR-PEEK was chosen for further investigation in this study.

Due the lack of differences in the shape of the models, investigation concentrated on evaluating the mechanical properties of the materials. As in previous studies [14, 19, 20], 100 N was used as the value for a load applied in a vertical incidence on the tooth occlusal surface, which aims to simulate the real function situation. There are no available random clinical studies regarding the influence of controlled or standardized loads on the peri-implant bone. Clinical quantification of the natural sense and value of occlusal loads is certainly difficult [19]. The bone tissue is known to be more resistant to the compressive loads, less resistant to the tensile loads, and even less resistant to the loads of shear [21]. However, determination of respective load parameters is perhaps the most important process, considering the implant in function and the osseous remodeling, the distinct effect of the traction and compression loads in this process have not been thoroughly investigated [22].

Some results [14, 23, 24] have indicated that the peri-implant bone remodeling may influence the load distribution even after the implant addition. The models from this study were constructed under ideal situation, considering the expected normal adaptation of the osseous level around the neck of a standard implant, within cortical bone the results were a higher concentration of the loads in the osseous cervical portion, and a slightly higher intensity in

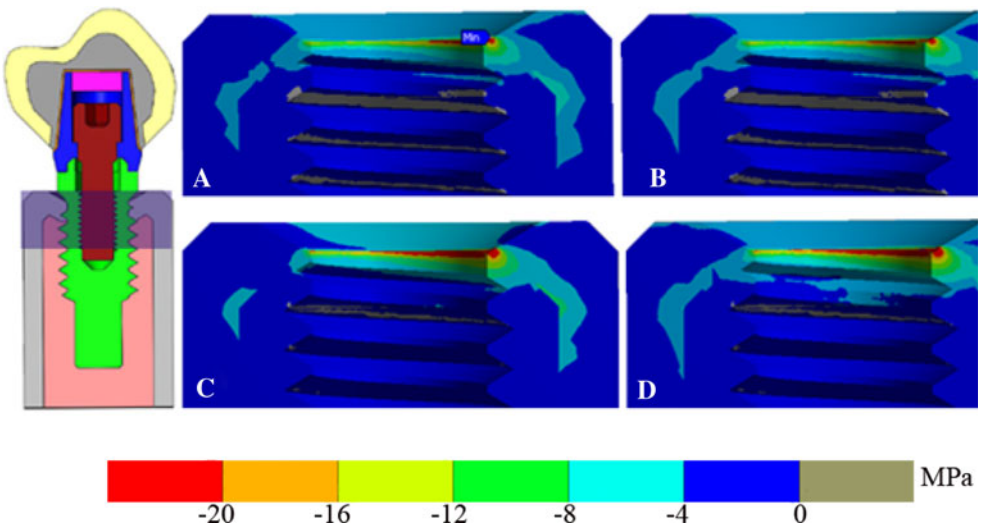

Fig. 3 Simulation result of the compression load only, minimum principal stress, with prominence for the area of higher concentration of the stress in the implant neck. *A* titanium implant and abutment, *B* titanium implant and CFR-PEEK abutment, *C* CFR-PEEK implant and titanium abutment, and *D* CFR-PEEK implant and abutment

Table 3 Results of the stress peaks in the different structures of the model (MPa)

	Von Mises implant	Von Mises abutment	Tensile Cortical/medullar	Compression Cortical/medullar
Model A or control (1 + 3)	76.46	41.76	32.70/2.48	81.14/3.19
Model B (1 + 4)	74.70	33.82	32.70/2.47	81.04/3.19
Model C (2 + 3)	85.54	41.32	27.77/4.22	89.47/3.58
Model D (2 + 4)	86.61	33.96	27.90/4.2	86.57/3.6

1 titanium implant *2* cfr-peek implant *3* titanium abutment *4* cfr-peek abutment

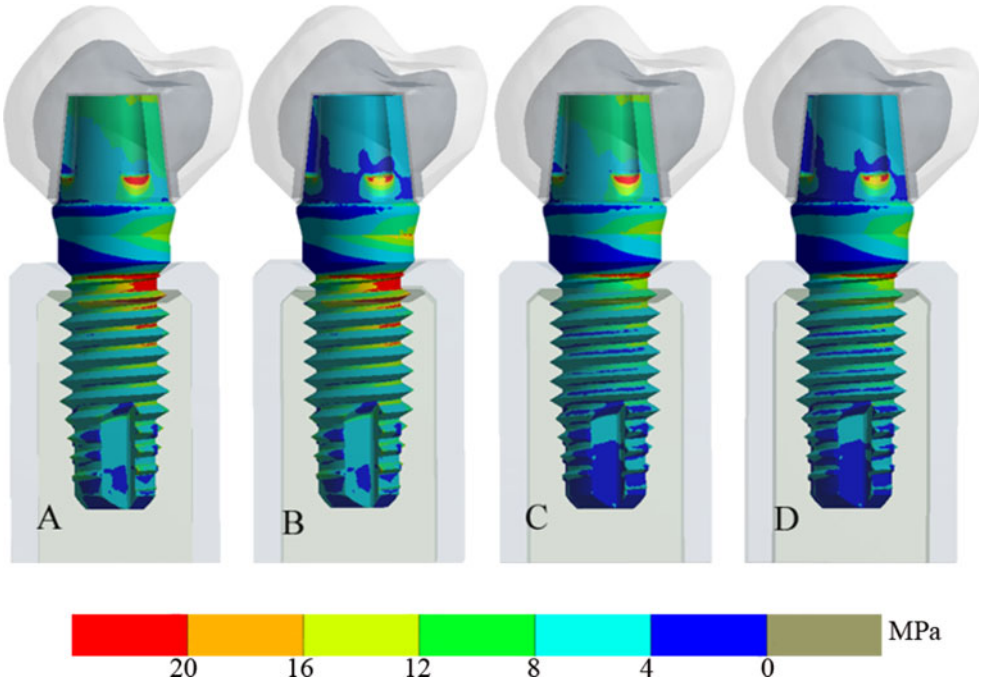

Fig. 4 Von Mises stress comparison among the implants and abutments. *A* titanium implant and abutment, *B* titanium implant and CFR-PEEK abutment, *C* CFR-PEEK implant and titanium abutment, and *D* CFR-PEEK implant and abutment

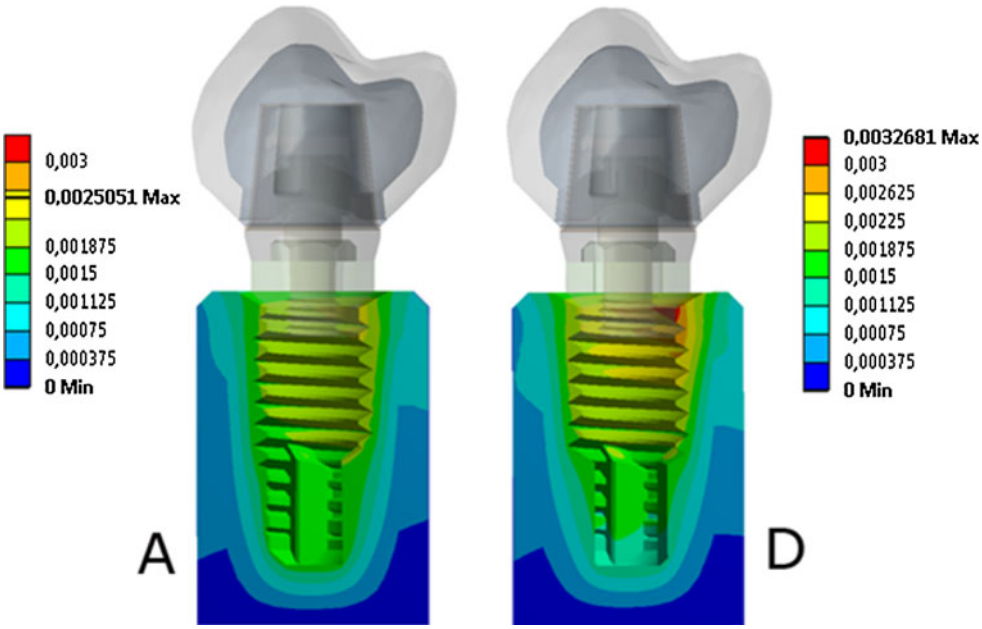

Fig. 5 Total deformation comparison with scale in millimeters. *A* titanium implant and abutment, and *D* CFR-PEEK implant and abutment. Observe the biggest deformations in the cervical region and the smallest ones in the apical of the implant in model *D*

Table 4 Results of the tension peaks in the different structures of the model with oblique load direction. (MPa)

	Von Mises implant	Von Mises abutment	Tensile Cortical/medullar	Compression Cortical/medullar
Model A or control (1 + 3)	171.42	84.82	22.02/2.65	146.26/3.95
Model B (1 + 4)	172.02	69.96	21.85/2.65	146.04/3.96
Model C (2 + 3)	188.95	84.17	58.82/4.90	177.81/6.42
Model D (2 + 4)	189.72	69.41	57.53/4.89	177.58/6.44

1 titanium implant *2* cfr-peek implant *3* titanium abutment *4* cfr-peek abutment

the CFR-PEEK implants (Table 3). These effects were demonstrated in similar studies [14, 25, 26] and may result of implant shape [26–28] or the highest resistance offered by the cortical bone in this area [29]. A stress concentration tendency in the implant neck of the different models was determinate through qualitative and quantitative analysis by the Von Mises criterion (Fig. 4 and Table 3), which is in agreement with the results of previous studies [30, 31]. However, smaller load transfer by the CFR-PEEK implant body with a higher load concentration was observed in a smaller area of the neck. In the titanium implants models the loads were transmitted in a more homogenous manner.

The study of the predicted deformations (Fig. 5) allows for a greater understanding of the stress distribution patterns presented by the different models. When model D with CFR-PEEK implant and abutment was simulated, the cervical portion of the implant suffered more deformation than model A with titanium implant and abutment. Consequently, model D had a higher displacement that generated higher stress (Table 3). This result confirms that micromovements of the dental implant are harmful for the support bone [26, 32, 33]. CFR-PEEK presents better results than titanium in terms of orthopedic applications [15, 16], due to decreased rigidity of this material. A higher deformation following spine movement increases the stress distribution area and reduces the load concentration. The bonding between implant and bone is rigid in dental implantodontics and therefore, does not allow for expansion by deformation. Such deformation is inherent in CFR-PEEK and presents a different functional behavior that significantly concentrates more stress in the implant neck. This was an unexpected result, since a more homogenous distribution of the stresses through the implant body was thought to diminish the stress at the implant and bone interface.

Regarding the prosthetic components, the stress distribution was equivalent for each material without any significant alteration in relation to the adjacent implants and without any influence on the load transfer to the peri-implant bone. However, it was expected a better load distribution to the implant/abutment by the CFR-PEEK abutments, once this material has an inferior young modulus than titanium. This same result was found in a previous study that tested polyoxymethylene modeled abutments and also in another experiment [34] that evaluated the stress distribution by photoelastic analysis. The result that a non-axial load is more harmful to the dental implants than an axial load is supported by previous studies [29, 34] utilizing 3D finite element analysis, and non-axial loads were determined to result in higher stress levels in the peri-implant bone than the axial loads. The same was observed in a study with finite element study, as the stress concentration in the bone and components of the implant system was determined to be higher when subjected to sidelong loads than vertical loads. Our results presented here confirmed this data when the simulation was performed with the obliqual load, as shown in Table 4.

5 Conclusion

The titanium implant distributes the stresses in a more homogenous manner in relation to the CFR-PEEK implant due to the smaller deformation of this material.

The CFR-PEEK implant did not present any advantages in relation to the titanium implant regarding stress distribution to the peri-implant bone.

References

1. Cook SD, Rust-Dawicki AM. Preliminary evaluation of titanium coated PEEK dental implants. J Oral Implantol. 1995;21:176–81.
2. Fujihara K, Huang ZM, Ramakrishna S, Satknanantham K, Hamada H. Performance study of braided carbon/PEEK composite compression bone plates. Biomaterials. 2003;24:2661–7.
3. Fujihara K, Huang ZM, Ramakrishna S, Satknanantham K, Hamada H. Feasibility of knitted carbon/PEEK composites for orthopedic bone plates. Biomaterials. 2004;25:3877–85.
4. Skinner HB. Composite technology for total hip arthroplasty. Clin Orthop Relat Res. 1988;235:224–36.
5. Wenz LM, Merritt K, Brown SA, Moet A, Steffee AD. In vitro biocompatibility of polyetheretherketone and polysulfone composites. J Biomed Mater Res. 1990;24:207–15.
6. Hunter A, Archer CW, Walker PS, Blunn GW. Attachment and proliferation of osteoblasts and fibroblasts on biomaterials for orthopaedic use. Biomaterials. 1995;16:287–95.
7. Morrison C, Macnair R, MacDonald C, Wykman A, Goldie I, Grant MH. In vitro biocompatibility testing of polymers for orthopaedic implants using cultured fibroblasts and osteoblasts. Biomaterials. 1995;16:987–92.

8. Lin TW, Corvelli AA, Frondoza CG, Roberts JC, Hungerford DS. Glass PEEK composite promotes proliferation and osteocalcin production of human osteoblastic cells. J Biomed Mater Res. 1997;36:137–44.
9. Katzer A, Marquardt H, Westendorf J, Wening JV, von Foerster G. Polyetheretherketone—cytotoxicity and mutagenicity in vitro. Biomaterials. 2002;23:1749–59.
10. Scotchford CA, Garle MJ, Batchelor J, Bradley J, Grant DM. Use of a novel carbon fibre composite material for the femoral stem component of a THR system: in vitro biological assessment. Biomaterials. 2003;24:4871–9.
11. Sheets CG, Earthmann JC. Natural intrusion and reversal in implant assisted prosthesis; evidence of and a hypothesis for the occurrence. J Prosthet Dent. 1993;70:513–20.
12. Anusavice KJ. Phillips' science of dental materials. 11th ed. St Louis: Sanders; 2003.
13. Tillitson EW, Craig RG, Peyton FA. Friction and wear of restorative dental materials. J Dent Res. 1971;50:149–54.
14. Kitamura E, Stegaroiu R, Nomura S, Miyakawa O. Biomechanical aspects of marginal bone resorption around osseointegrated implants: considerations based on a three-dimensional finite element analysis. Clin Oral Implants Res. 2004;15:401–12.
15. Kurtz SM, Devine JN. PEEK biomaterials in trauma, orthopedic and spinal implants. Biomaterials. 2007;28:4845–69.
16. Toth JM, Wang M, Estes BT, Scifert JL, Seim HB, Turner AS. Polyetheretherketone as a biomaterial for spinal applications. Biomaterials. 2006;27:324–34.
17. Brantigan JW, Neidre A, Toohey JS. The Lumbar I/F Cage for posterior lumbar interbody fusion with the variable screw placement system: 10-year results of a Food and Drug Administration clinical trial. Spine J. 2004;4:681–8.
18. Akhavan S, Matthiesen MM, Schulte L, Penoyar T, Kraay MJ, Rimnac CM, Goldberg VM. Clinical and histologic results related to a lowmodulus composite total hip replacement stem. J Bone Joint Surg Am. 2006;88:1308–14.
19. Isidor F. Influence of forces on peri-implant bone. Clin Oral Implants Res. 2006;17(Suppl 2):8–18.
20. Williams KR, Edmundson JT, Rees JS. Finite element stress analysis of restored teeth. Dent Mater. 1987;3:200–6.
21. Misch CE, Suzuki JB, Misch-Dietsh FM, Bidez MW. A positive correlation between occlusal trauma and peri-implant bone loss: literature support. Implant Dent. 2005;14:108–16.
22. Hobkirk JA and Wiskott HW. Biomechanical aspects of oral implants: consensus report of Working Group I. Clin Oral Implants Res. 2006;17(Suppl 2):52–4.
23. Petrie CS, Williams JL. Comparative evaluation of implant designs: influence of diameter, length, and taper on strains in the alveolar crest. A three-dimensional finite element analysis. Clin Oral Implants Res. 2005;16:486–94.
24. Kitamura E, Stegaroiu R, Nomura S, Miyakawa O. Influence of marginal bone resorption on stress around an implant–a three dimensional finite element analysis. J Oral Rehabil. 2005;32:279–86.
25. Bidez MW, Misch CE. Issues in bone mechanics related to oral implants. Implant Dent. 1992;1:289–94.
26. Bozkaya D, Muftu S, Muftu A. Evaluation of load transfer characteristics of five different implants in compact bone at different load levels by finite elements analysis. J Prosthet Dent. 2004;92:523–30.
27. Siegele D, Soltesz U. Numerical investigations of the influence of implant shape on stress distribution in the jaw bone. Int J Oral Maxillofac Implants. 1989;4:333–40.
28. Geng JP, Q. Ma QS, Xu W, Tan KB, Liu GR. Finite element analysis of four threat-form configurations in a stepped screw implant. J Oral Rehabil. 2004;31:233–9.
29. Meyer U, Vollmer D, Runte C, Bourauel C, Joos U. Bone loading pattern around implants in average and atrophic edentulous maxillae: a finite-element analysis. J Maxillofac Surg. 2001;29:100–5.
30. Koca OL, Eskitascioglu G, Usumez A. Three-dimensional finite-element analysis of functional stresses in different bone locations produced by implants placed in the maxillary posterial region of the sinus floor. J Prosthet Dent. 2005;93:38–44.
31. Zampelis A, Rangert B, Heijl L. Tilting of splinted implants for improved prosthodontic support: a two-dimensional finite element analysis. J Prosthet Dent. 2007;97:535–43.
32. Natali AN, Carniel EL, Pavan PG. Investigation of bone inellastic response in interaction phenomena with dental implants. Dent Mater. 2008;24:561–9.
33. Cehreli M, Duyck J, De Cooman M, Puers R, Naert I. Implant design and interface force transfer: a photoelastic and strain-gauge analysis. Clin Oral Implants Res. 2004;15:249–57.
34. Sutpideler M, Eckert SE, Zobitz M, An KN. Finite element analysis of effect of prosthesis height, angle of force application, and implant offset on supporting bone. Int J Oral Maxillofac Implants. 2004;19:819–25.